Vegetation (Longman, London, 1974).
12. Soil fractions were prepared as follows: macroscopic organic matter was removed by hand, the soil gently ground in a mortar, and sieved. The <355-μm fraction (10 g) was treated with 1 M HCl at 25°C for 15 hours and rinsed to pH 3 by centrifugation with distilled water. Carbonate-free whole soil (1 g) was reserved; the remainder was treated with 50 ml of 0.125 M NaOH for 15 hours at 25°C, with constant agitation on a reciprocal shaker. The supernatant (humic acids) was reserved, and the treatment repeated. The residue (humin) was rinsed, acidified, rinsed to pH 3, and freeze-dried. The humic acid supernatants were precipitated by titration with HCl, centrifuged, and the residue rinsed to pH 3. This residue was redissolved in 25 ml of 0.125 M NaOH, centrifuged, and any pellet was discarded. The supernatant (purified humic acids) was reprecipitated, rinsed to pH 3, and freeze-dried. Plant leaves were sonicated in distilled water, dried at 70°C, and ground in a Wiley Mill. Organic carbon was converted to CO_2 by sealed tube combustion with CuO, Cu, and Ag foil for 3 hours at 860°C. The precision of $\delta^{13}C$ analysis is ±0.1 per mil (1 SD).
13. The $\delta^{13}C$ values of 41 paired whole soil and humic acid fractions are correlated ($r^2 = 0.988$); their mean difference is 0.09 ± 0.36 per mil (1 SD).
14. J. A. Matthews, in *Geomorphology and Soils*, K. S. Richards, R. R. Arnett, S. Ellis, Eds. (Allen & Unwin, London, 1985), pp. 269–288.
15. K. W. Butzer, G. L. Isaac, J. L. Richardson, C. K. Washbourne-Kamau, *Science* **175**, 1069 (1972).
16. J. L. Richardson and A. E. Richardson, *Ecol. Monogr.* **42**, 499 (1972); J. L. Richardson and R. A. Dussinger, *Hydrobiologia* **143**, 167 (1986); J. M. Maitima, *Quat. Res.* **35**, 234 (1991).
17. J. L. Richardson, *Palaeoecol. Africa* **6**, 131 (1972).
18. R. A. Perrott, *Nature* **325**, 89 (1987); D. M. Taylor, *Palaeogeogr. Palaeoclimatol. Palaeoecol.* **80**, 283 (1990).
19. A. C. Hamilton, D. Taylor, J. C. Vogel, *Nature* **320**, 164 (1986); in *Quaternary and Environmental Research on East African Mountains*, W. C. Mahaney, Ed. (Balkema, Rotterdam, 1989), pp. 435–463.
20. R. H. Blackburn, in *Politics and History in Band Societies*, R. B. Lee and E. Leacock, Eds. (Cambridge Univ. Press, Cambridge, 1982), pp. 283–305.
21. S. H. Ambrose, thesis, University of California, Berkeley (1984).
22. D. P. Gifford-González, *Azania* **20**, 69 (1985).
23. C. W. Marean, thesis, University of California, Berkeley (1990).
24. S. H. Ambrose and M. J. DeNiro, *Quat Res.* **31**, 407 (1989).
25. D. Schwartz, A. Mariotti, R. Lanfranchi, B. Guillet, *Geoderma* **39**, 97 (1986); J. Quade, T. E. Cerling, J. R. Bowman, *Nature* **342**, 163 (1989).
26. R. S. Dzurec *et al.*, *Oecologia* **66**, 17 (1985).
27. We thank the Office of the President and the National Museums of Kenya for permission to conduct field research and J. Hayes, C. Kabuye, and the staff of the East African Herbarium for plant identifications. T. Anderson, T. Cerling, T. Dillehay, D. Gillieson, L. Follmer, D. Johnson, and L. Norr provided useful comments. Supported by NSF grant BNS 87-07150 and the University of Illinois Research Board.

22 January 1991; accepted 12 June 1991

Atomic Force Microscopy and Dissection of Gap Junctions

JAN H. HOH, RATNESHWAR LAL,* SCOTT A. JOHN, JEAN-PAUL REVEL, MORTON F. ARNSDORF

An atomic force microscope (AFM) was used to study the structure of isolated hepatic gap junctions in phosphate-buffered saline (PBS). The thickness of these gap junctions appears to be 14.4 nanometers, close to the dimensions reported by electron microscopy (EM). When an increasing force is applied to the microscope tip, the top membrane of the gap junction can be "dissected" away, leaving the extracellular domains of the bottom membrane exposed. When such "force dissection" is performed on samples both trypsinized and fixed with glutaraldehyde, the hexagonal array of gap junction hemichannels is revealed, with a center-to-center spacing of 9.1 nanometers.

GAP JUNCTIONS CONSIST OF TWO apposed plasma membranes that contain an array of cell to cell channels (*1*). These channels form aqueous pores that allow the free passage of small molecules (<1 kD) in vertebrates and provide a low-resistance electrical pathway between cells (*2*). Proposed biological functions for gap junctions include regulation of growth, transmission of developmental signals, coordination of smooth muscle contraction, synchronization of myocardial contractions, and maintenance of metabolic homeostasis (*3*).

The structure of the gap junction has been studied extensively by physical and biochemical methods. It was first described by EM as a close membrane apposition (*4*) with a quasi-crystalline array of particles (*5*), and subsequently a gap between the membranes was defined (*1*). Models of the gap junction have been constructed with data from x-ray diffraction, EM, and Fourier-based three-dimensional reconstruction techniques (*6, 7*). In the current model, the gap junction is composed of two apposed membranes with a 2- to 3-nm gap between them and a closely packed array of cell-cell channels. The most regular samples show hexagonal packing with a lattice constant of 8 to 10 nm, but the degree of order varies depending on the preparation. Each channel is composed of two connexons, one from each membrane, aligned head-to-head across the gap. The connexon is shaped roughly as a cylinder 7.5 nm in height and 7 nm in diameter, with a 1.5- to 2.0-nm pore through the center. Each connexon exhibits sixfold symmetry and is thought to consist of six identical or homologous protein subunits.

The AFM has been used to image a number of biological specimens (*8–10*). Details of the operation of AFMs have been presented (*8, 11, 12*). We have used an AFM equipped with a fluid cell to probe the structure and organization of isolated gap junctions adsorbed to glass in PBS (*13*), and we have also used the AFM to manipulate these membranes.

Gap junctions from rat liver were isolated as membrane pairs, often referred to as plaques, with densely packed cell to cell channels (*14*). These plaques, imaged under PBS by atomic force microscopy, appear to be similar in general shape and distribution to ones seen by EM (Fig. 1, A and B). They are flat structures, 0.5 to 1 μm in size, with irregular edges and are 14.4 nm thick (Fig. 1C). Occasionally a step of 6 to 7 nm is seen at the edge of a plaque that either represents a single membrane from a gap junctional plaque or a piece of nonjunctional membrane attached to the gap junction. The surface of the gap junction has height variations of ~1 nm, but sometimes bumps 50 to 100 nm in width and several nanometers in height are seen. At high magnification, the surface has no discernible regular features and is smoothly undulating. High-magnification images of the glass itself are remarkably smooth, with z variation of only 1 to 2 nm and no detectable regular pattern (Fig. 1D).

Glutaraldehyde fixation of hepatic gap junctions does not result in any discernible changes in morphology. Interestingly, all of the samples that were glutaraldehyde-fixed were more easily scraped off the glass substrate. This result may be attributable to the reaction of glutaraldehyde with amino groups of molecules such as phospholipids and proteins. Reaction of these molecules with glutaraldehyde would reduce the total positive charge of the gap junction membrane and thereby reduce the strength of the electrostatic interactions between the gap junction and the negatively charged glass. The adsorption of purple membranes to mica requires positively charged membranes (*10*).

We examined the effect of force on the structure and appearance of the gap junction. Samples were imaged in PBS in an increasing force series from less than 1 nanonewton (nN) to ~15 nN. After a gap

J. H. Hoh, S. A. John, J.-P. Revel, Division of Biology, California Institute of Technology, Pasadena, CA 91125. R. Lal and M. F. Arnsdorf, Section of Cardiology, Department of Medicine, University of Chicago, Chicago, IL 60637.

*To whom correspondence should be addressed.

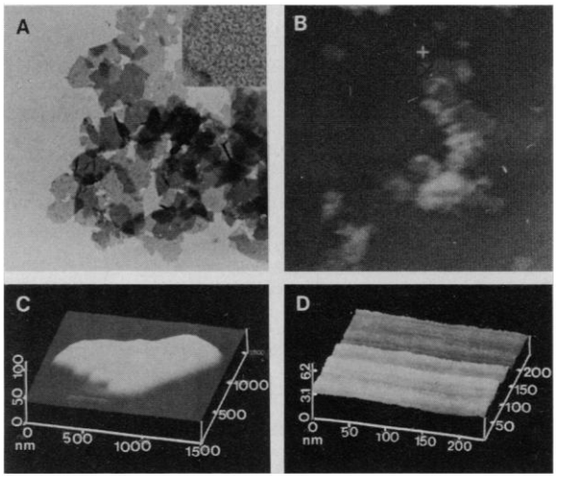

Fig. 1. Low-magnification images of isolated rat liver gap junctions (**A**) by EM of negatively stained samples with phosphotungstic acid and (**B**) in PBS taken with the AFM. The high magnification inset in (A) shows the connexons in the gap junction plaques as seen by EM. The gap junctions in the AFM appear similar in shape and distribution to ones in the EM images. Also shown are (**C**) a single gap junction plaque at an intermediate magnification and (**D**) a surface view of a high-magnification image of the glass cover slip. The glass is extremely smooth but does have a ripple that is 1 to 2 nm in the scan direction. The gap junction plaque has the typical shape, is ~15 nm thick, and shows the bumps that are sometimes present on the gap junction surface. The scan direction in all images in this report is along the *x*-axis. Gap junctions containing 200 to 300 ng of Cx32 protein were diluted into 50 to 75 μl of PBS on a glass cover slip (*24*), adsorbed for 10 to 20 min, and subsequently washed twice in 20 ml of PBS for 5 min. Samples were stored for up to 8 hours in PBS before being imaged. Temperature near the AFM was 21° to 25°C. A NanoScope II equipped with an 18 by 18 μm AFM stage and a fluid cell was used for imaging (*25*). Cantilevers were V-shaped, with a spring constant of 0.38 N/m and pyramidal tips (*25, 26*). In addition to the gold coating on the top surface, the bottom surface, including the tip, was coated with a thin layer of chromium by the manufacturer. In order to control and minimize the amount of force the sample was subjected to, we routinely engaged the tip onto a 49 by 49 nm scan area in the center of the field. The force was then adjusted to ~1 nN, and the scan area was gradually enlarged until it included a sample to be imaged. The force during imaging was always monitored closely and assessed within 15 to 30 s of acquiring an image.

junction was located at a low force, the plaque appeared to be stable for several sweeps of the tip. Remarkably, upon an increase in the force, the top membrane of the gap junction became distorted and, after several sweeps of the tip, would be completely removed, exposing a new surface that we believe is the extracellular surface of the bottom membrane of the gap junction (Fig. 2). During this "force dissection," the thickness of the native plaques changed from 14.4 nm for the double bilayer to 6.4 nm for the single bilayer (compare Fig. 2A with 2D or 2E with 2H). The remaining half of the junction plaque could only be removed at extremely high forces, suggesting that the interactions between the glass and the gap junction are significantly stronger than those between the two membranes of the gap junction. Force dissection was also carried out on both trypsinized and glutaraldehyde-fixed samples, with similar results.

Splitting of gap junctions has been accomplished in a variety of ways (*15, 16*). Researchers have used such junctions to demonstrate the extracellular localization of specific segments of the connexins by label-

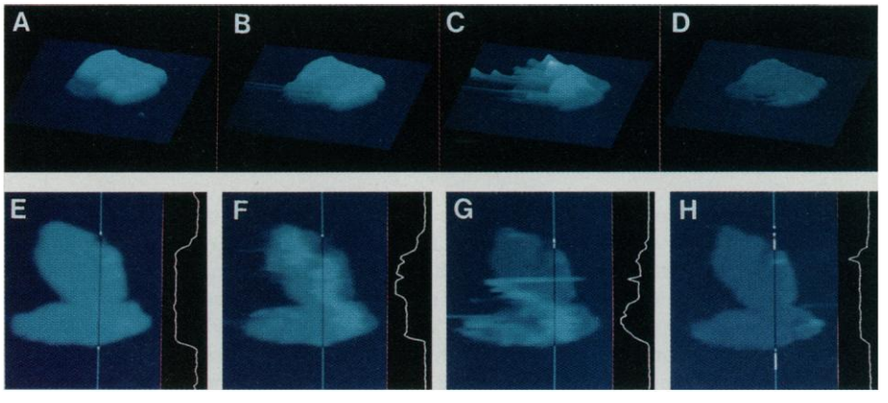

Fig. 2. Force dissection with the AFM of gap junction membranes in PBS adsorbed to glass. The top row of images shows a surface view of a gap junction plaque subjected to a sequential series of scans at increasing forces of (**A**) 0.8 nN, (**B**) 3.6 nN, (**C**) 6.1 nN, and (**D**) 9.6 nN. The field size is 1.5 μm by 1.5 μm and the plaque image is ~15 nm thick. A piece of single membrane is attached to one edge of the plaque. At low force the shape of the plaque is stable for several scans, but as the force is increased the top membrane begins to smear from right to left and is eventually removed completely, leaving the extracellular side of the 7-nm-thick bottom membrane exposed. The second series of images shows a top view of another gap junction plaque as it is subjected to sequential scans at increasing forces of (**E**) 0.8 nN, (**F**) 3.1 nN, (**G**) 10.1 nN, and a repeat scan at (**H**) 10.1 nN. The field size is 1.5 μm by 1.5 μm and the line cut marked on each image is shown on the right. These line cuts show clearly how the top membrane is removed at higher forces, reducing the thickness of the structure to one-half that of the original. The thickness of the structure is about 15 nm in the first image (E) and about 7 nm in the last (H).

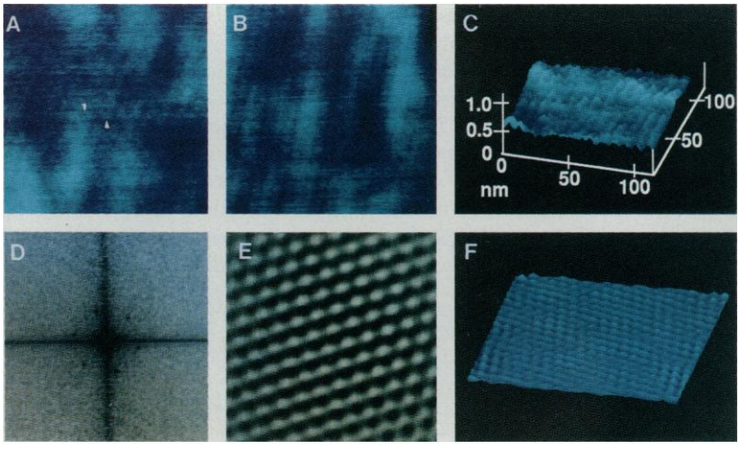

Fig. 3. Imaging of extracellular surface and connexons of a gap junction plaque that has been both trypsinized and glutaraldehyde-fixed (*27*). (**A**) High-magnification (120 nm wide) images show the hexagonal array of connexons. The connexons appear to be ~4 to 6 nm in diameter and sometimes have a depression in the center, indicated by arrows, which may represent part of the pore of the channel. (**B**) In some samples a rowlike appearance was apparent. (**C**) The surface view shows the connexons protruding approximately 0.4 to 0.5 nm. Images (A) through (E) were all plane-fitted but not processed further. (**D**) Fourier transforms reveal a distinct hexagonal array with a 9.1-nm center-to-center spacing (*19*). The hexagonal pattern is only shown to one order in this sample, although second-order spots are often seen. (**E**) A top view of the filtered inverse Fourier transform (91 by 91 nm) clearly shows the hexagonal packing. (**F**) The surface view of a filtered inverse Fourier transform (175 by 195 nm) also shows the hexagonal pattern but reveals some irregularity in the packing.

ing with antibodies against specific peptides (*16, 17*). However, the conditions for splitting are somewhat harsh, and it is often difficult to know morphologically which side is which in the resulting single membranes. Force dissection has the advantage of giving access to the extracellular domains in a controlled fashion and making them available for immediate experimental manipulation.

The observation that fixed gap junctions can be force-dissected at forces similar to those required for unfixed material suggests that glutaraldehyde does not cause the formation of cross-links across the gap. The phospholipid head groups in the plane of the membrane are separated by a 2- to 3-nm gap and are therefore unlikely to be cross-linked. However, the extracellular domains in connexin-32, the major hepatic gap junction protein, span the gap to interact with the identical domains in the opposing connexon. These extracellular domains have several residues that could be cross-linked with glutaraldehyde. Because there is apparently little or no cross-linking across the gap, these residues are likely neither near each other in the connexon-connexon interactions nor accessible to the glutaraldehyde.

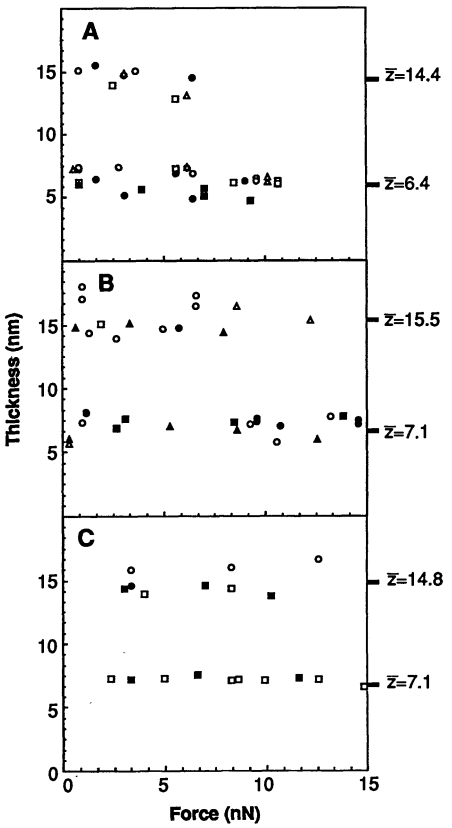

Fig. 4. Force versus thickness distributions for (**A**) native, (**B**) trypsinized, and (**C**) glutaraldehyde-fixed gap junctions (*27*). Single gap junction plaques were imaged with increasing and decreasing series of force. At each force an image of a plaque was acquired, and the thickness was measured from line cuts of each plaque taken at 0°, 90°, and 45° from the scan direction. Three measurements from each cut were taken. There was no significant difference in the thickness measured at the different angles, so all measurements from a single plaque at a given force were averaged ($\bar{z}$). Each symbol in a given graph represents a different plaque.

We have looked for the cell-cell channels on the surface of gap junctions under a variety of conditions. In intact gap junctions there is no substructure and the surface appears smooth, as shown by EM images of deeply etched samples (*18*). However, a distinct hexagonal pattern is revealed on the surface exposed by force dissection of gap junction plaques that have been trypsinized and glutaraldehyde-fixed (Fig. 3A). This hexagonal array is remarkably similar to the pattern of cell-cell channels seen in negatively stained isolated gap junctions in EM (*7*). We believe that it represents an image of connexons protruding into the extracellular space. The connexons appear 4 to 6 nm in diameter, which is less than the diameter suggested by current models (*6, 7*), and protrude 0.4 to 0.5 nm from the surface of the plaque (Fig. 3C). Some connexons have a small depression in the center that could represent part of the channel pore.

Sometimes the surface of gap junction hemichannels appeared to be in rows (Fig. 3B). This is also evident in the Fourier transform, where the intensity of the six symmetrical spots sometimes varied, suggesting a more defined order in one direction. These rows were not an artifact of the scanning, because the rows moved relative to the scan direction when it was altered up to 35°.

A two-dimensional Fourier transform of the AFM image produces a distinct sixfold symmetry in the frequency domain (Fig. 3D). The center-to-center spacing for the hexagonal array determined from the Fourier transform is 9.1 nm (*19*). This spacing is extraordinarily close to values obtained by x-ray diffraction and EM (*6, 7*). The sixfold pattern is clearly visible to one order, and second-order spots are often seen, suggesting that there is short-range disorder in the hexagonal array, which is also shown in the filtered image (Fig. 3E). Previous data suggest that the degree of order in the hexagonal arrays of cell-cell channels varies depending on the preparation, and there have been suggestions that the variation in packing has physiological significance (*20*).

We performed measurements on gap junction plaques in a series of ascending and descending forces, although the force dissection somewhat complicated the measurement of the thickness of gap junctions and the effect of force. In cases where force dissection occurred, the descending series would often include only the 7-nm profiles. These measurements were carried out for isolated native hepatic gap junctions, trypsinized gap junctions, and glutaraldehyde-fixed gap junctions (Fig. 4). We found no statistically significant effect of force on the thickness of any of the gap junction samples, and there is no significant effect of the treatments. The thickness distribution versus force shows the full and half thicknesses of the plaques, and, because there is no observable effect of force, all of the measurements were combined. The means of thicknesses (± SD) are 14.4 ± 0.9 nm and 6.4 ± 0.8 nm for native plaques, 15.5 ± 1.3 nm and 7.1 ± 0.7 nm for trypsinized plaques, and 14.8 ± 1.0 nm and 7.1 ± 0.3 nm for glutaraldehyde-fixed plaques. The thicknesses of native gap junctions we have measured are in general agreement with the thickness of 15 to 18 nm determined by x-ray diffraction and EM (*21*). The apparent thickness of purple membranes depends on the substrate used (*10*). Until the basis for this substrate dependence is understood, the significance of the absolute measurements reported here will not be known.

Trypsinization is known to remove 60 to 70 amino acids from the cytoplasmic surface of Cx32 and cleave the protein into two 10-kD fragments that contain the four transmembrane domains and the two extracellular loops (*22*). The AFM images of trypsinized and untrypsinized gap junctions appear identical, and there is no apparent change in shape or thickness. One might have expected intuitively that the thickness would have been affected by the removal of protein from the surface, but this is not the case. In contrast, native cardiac gap junctions that have a larger cytoplasmic protein domain are significantly thicker than hepatic gap junctions but are reduced to a thickness of 14 to 15 nm upon trypsinization (*23*). This result would suggest that there is not enough protein mass removed from the hepatic gap junction by trypsinization to affect the thickness or that the protein removed was closely associated with the membrane and thus did not contribute significantly to the overall thickness of the gap junction.

REFERENCES AND NOTES

1. J.-P. Revel and M. Karnovsky, *J. Cell Biol.* **33**, C7 (1967).
2. J. Flagg-Newton, I. Simpson, W. R. Loewenstein, *Science* **205**, 404 (1979).
3. E. L. Hertzberg, R. G. Johnson, *Modern Cell Biology: Gap Junctions* (Liss, New York, 1988).
4. M. M. Dewey and L. Barr, *Science* **137**, 670 (1962).
5. H. E. Karrer and J. Cox, *J. Biophys. Biochem. Cytol.* **8**, 135 (1960).
6. L. Makowski, D. L. D. Caspar, W. C. Philips, D. A.

Goodenough, *J. Cell Biol.* **74**, 629 (1977); L. Makowski, in *Gap Junctions*, M. V. L. Bennett and D. C. Spray, Eds. (Cold Spring Harbor Laboratory, Cold Spring Harbor, NY, 1985), pp. 5–12.
7. P. N. T. Unwin and G. Zampighi, *Nature* **283**, 545 (1980).
8. B. Drake *et al.*, *Science* **243**, 1586 (1989).
9. R. D. Edstrom *et al.*, *Biophys. J.* **58**, 1437 (1990).
10. H.-J. Butt *et al.*, *ibid.*, p. 1473.
11. G. Binnig, C. F. Quate, C. Gerber, *Phys. Rev. Lett.* **56**, 930 (1986).
12. S. A. C. Gould *et al.*, *J. Vac. Sci. Technol. A* **8**, 369 (1990); D. Rugar and P. Hansma, *Phys. Today* **43**, 23 (October 1990).
13. Phosphate-buffered saline was 137 mM NaCl, 2.7 mM KCl, 1.5 mM KH_2PO_4, and 4.3 mM Na_2HPO_4 at pH 7.2.
14. We have used a routinely applied isolation method similar to ones described [M. E. Finbow, S. B. Yancey, R. G. Johnson, J. Revel, *Proc. Natl. Acad. Sci. U.S.A.* **77**, 970 (1980); D. Henderson, H. Eibl, K. Weber, *J. Mol. Biol.* **132**, 193 (1979)]. These gap junctions were determined to be highly purified on the basis of EM and polyacrylamide gel electrophoresis analysis. Animals used for the preparation of gap junctions were treated in accordance with institutional guidelines.
15. C. K. Manjunath, G. E. Goings, E. Page, *Biochem. J.* **205**, 189 (1982).
16. D. A. Goodenough, D. L. Paul, L. Jesaitis, *J. Cell Biol.* **107**, 1817 (1988).
17. D. W. Laird and J.-P. Revel, *J. Cell Sci.* **97**, 109 (1990).
18. N. Hirokawa and J. Heuser, *Cell* **30**, 395 (1982).
19. The lattice constant (L) is determined from the Fourier transform by $L = (1/\sin 120°)(1/a^*)$.
20. G. Bernardini and C. Peracchia, *Invest. Ophthalmol. Vis. Sci.* **21**, 291 (1981); G. E. Sosinsky, T. S. Baker, D. L. D. Caspar, D. A. Goodenough, *Biophys. J.* **58**, 1213 (1990).
21. G. E. Sosinsky *et al.*, *Biophys. J.* **53**, 709 (1988).
22. B. J. Nicholson *et al.*, *Proc. Natl. Acad. Sci. U.S.A.* **78**, 7594 (1981).
23. S. A. John *et al.*, unpublished observation.
24. Glass cover slips (no. 1 thickness) (Fisher Scientific) were mounted on metal stubs obtained from Digital Instruments (Santa Barbara, CA). Cover slips were cleaned with a mild detergent and rinsed with distilled water. All of the solutions used for imaging were filtered through a 0.2-μm filter to remove large debris.
25. Imaging was carried out at Imaging Services (Truckee, CA). The NanoScope II and cantilevers were from Digital Instruments. The stage we used was calibrated at Digital Instruments on a diffraction grating (xy) and by interferometry (z).
26. T. R. Albrecht, S. Akamine, T. E. Carver, C. F. Quate, *J. Vac. Sci. Technol. A* **8**, 3386 (1990).
27. Trypsinization was carried out in PBS at an enzyme to substrate ratio of 1:10 for 2 hours at 25°C after which an excess of soybean trypsin inhibitor was added. The gap junctions were pelleted at 14,000g for 30 min and the supernatant was aspirated. Complete digestion was assessed by SDS–polyacrylamide gel electrophoresis, which showed the 10-kD band known to result from trypsinization. The trypsinized gap junctions were resuspended in PBS and stored at less than −20°C until used. Fixation was carried out on trypsinized gap junctions adsorbed to glass by submersion of the entire stub with the cover slip and sample in 1% glutaraldehyde in PBS at room temperature for 20 to 30 min. The gap junctions were subsequently rinsed several times in PBS and kept in PBS at room temperature for up to several hours.
28. Supported by NIH grants R37 HL21788 to M.F.A. and HL37109 and BRSG-RR07003 to J.-P.R. We thank B. Drake of Imaging Services for his help with the operation of the AFM; R. Johnson, P. Lampke, K. Puranam, and B. Yancey for comments on the manuscript; P. Bjorkman for help in interpreting the Fourier transform; and M. Jentoft-Nilsen for helpful discussions.

25 February 1991; accepted 12 June 1991

A Combinatorial Approach Toward DNA Recognition

DEHUA PEI, HELLE D. ULRICH, PETER G. SCHULTZ*

A combinatorial approach has been used to identify individual RNA molecules from a large population of sequences that bind a 16–base pair homopurine-homopyrimidine DNA sequence through triple-helix formation. Fourteen of the seventeen clones selected contained stretches of pyrimidines highly homologous to the target DNA sequence (T·AT and C^+·GC). In addition, these RNA molecules contained hairpin loops, interior loops, and nonstandard base triplets [C^+(or C)·AT, U·GC, G·GC, and A·AT] at various positions. Affinity cleavage experiments confirmed the ability of selected sequences to bind specifically to the target DNA. Systematic variation in both the target DNA sequence and buffer components should provide increased insight into the molecular interactions required for triple-helix–mediated recognition of natural DNA.

THE POWER OF COMBINATORIAL strategies for generating molecules with novel properties has been exploited in the generation of catalytic antibodies (*1*) and more recently in the study of protein-ligand interactions (*2–5*). We report application of this approach to the molecular recognition of double-helical DNA through the synthesis and screening of large RNA libraries for selective triple-helix formation. The sugar-phosphate backbone of nucleic acids provides a natural framework for building specific hydrogen-bonding interactions with functional groups in the major groove of DNA (*6*). This structural motif, however, is currently limited to the recognition of predominantly homopurine-homopyrimidine tracts of DNA. Polypyrimidine oligonucleotides bind specifically in the major groove, parallel to the purine strand, through Hoogsteen T·AT and C^+·GC base triplets (*7, 8*). Polypurine oligonucleotides bind in the major groove, parallel to the pyrimidine strand, through G·GC and A·AT triplets (*9*). Recently, it has been shown that a G·TA triplet can also be formed in a polypyrimidine oligonucleotide, although the interaction is considerably weaker than the T·AT triplet (*10*). Given the conformational flexibility associated with nucleic acids, as well as the effects of pH, salt, and small molecules on nucleic acid structure, it was of interest to determine whether additional hydrogen-bonding schemes might be associated with triple-helix formation. The extension of triple-helix formation to the recognition of mixed DNA sequences would likely find applications in the analysis of nucleic acid structure and function (*11*) as well as in the development of therapeutic agents based on selective gene inactivation (*12*).

Because a general solution to triple-helix–mediated recognition of natural DNA sequences might involve relatively complex rules (including context effects, looped structures, and conformational isomers), we chose a strategy that samples large numbers of diverse sequences for binding to a defined DNA duplex. Analysis of those sequences that form the most stable triple-stranded structures, coupled with systematic variations in the target sequence, should provide increased insight into the molecular interactions responsible for triple-helix formation. In order to test the feasibility of this approach, an RNA library has been generated and screened against a homopurine-homopyrimidine target DNA, for which the recognition "rules" are known (T·AT and C^+·GC) (*7, 8*).

The library of randomized RNA molecules was generated from a 106-nucleotide (nt) DNA template containing: (i) a T7 promoter sequence; (ii) a 16-nt priming site for the polymerase chain reaction (PCR); (iii) a 50-nt random sequence (synthesized from an equimolar mixture of the four bases); and (iv) another 23-nt priming site for reverse transcription and PCR amplification of the in vitro transcripts (Fig. 1A) (*2, 3*). In vitro transcription of the template with a 33-nt primer (Fig. 1A) and T7 RNA polymerase (*13*) affords an 89-nt RNA transcript. Based on the amount of the DNA template used in the initial transcription reaction, the complexity of the RNA pool generated from this template is on the order of 10^{10} to 10^{12} individual primary sequences, a small fraction of all possible sequences (*3*). In addition to sequence diversity, randomized 50-nt oligoribonucleotides should be able to form a large number

Department of Chemistry, University of California, Berkeley, Berkeley, CA 94720.

*To whom correspondence should be addressed.